

REPORT DOCUMENTATION PAGE

Form Approved
OMB No. 0704-0188

Public reporting burden for this collection of information is estimated to average 1 hour per response, including the time for reviewing instructions, searching existing data sources, gathering and maintaining the data needed, and completing and reviewing this collection of information. Send comments regarding this burden estimate or any other aspect of this collection of information, including suggestions for reducing this burden to Department of Defense, Washington Headquarters Services, Directorate for Information Operations and Reports (0704-0188), 1215 Jefferson Davis Highway, Suite 1204, Arlington, VA 22202-4302. Respondents should be aware that notwithstanding any other provision of law, no person shall be subject to any penalty for failing to comply with a collection of information if it does not display a currently valid OMB control number. PLEASE DO NOT RETURN YOUR FORM TO THE ABOVE ADDRESS.

1. REPORT DATE (DD-MM-YYYY)	2. REPORT TYPE Technical Papers	3. DATES COVERED (From - To)
-----------------------------	------------------------------------	------------------------------

4. TITLE AND SUBTITLE	5a. CONTRACT NUMBER
	5b. GRANT NUMBER
	5c. PROGRAM ELEMENT NUMBER

Please see
attached

6. AUTHOR(S)	5d. PROJECT NUMBER 2302
	5e. TASK NUMBER MIG2
	5f. WORK UNIT NUMBER 346120

7. PERFORMING ORGANIZATION NAME(S) AND ADDRESS(ES) Air Force Research Laboratory (AFMC) AFRL/PRS 5 Pollux Drive Edwards AFB CA 93524-7048	8. PERFORMING ORGANIZATION REPORT
---	-----------------------------------

9. SPONSORING / MONITORING AGENCY NAME(S) AND ADDRESS(ES) Air Force Research Laboratory (AFMC) AFRL/PRS 5 Pollux Drive Edwards AFB CA 93524-7048	10. SPONSOR/MONITOR'S ACRONYM(S)
	11. SPONSOR/MONITOR'S NUMBER(S) Please see attached


12. DISTRIBUTION / AVAILABILITY STATEMENT
Approved for public release; distribution unlimited.

13. SUPPLEMENTARY NOTES

14. ABSTRACT

20030128 228

15. SUBJECT TERMS

16. SECURITY CLASSIFICATION OF:			17. LIMITATION OF ABSTRACT 	18. NUMBER OF PAGES	19a. NAME OF RESPONSIBLE PERSON Leilani Richardson
a. REPORT Unclassified	b. ABSTRACT Unclassified	c. THIS PAGE Unclassified			19b. TELEPHONE NUMBER (include area code) (661) 275-5015

2302MIG2 DTW

FILE

MEMORANDUM FOR PRS (In-House Publication)

FROM: PROI (STINFO)

16 Mar 2001

SUBJECT: Authorization for Release of Technical Information, Control Number: **AFRL-PR-ED-TP-2001-061**
Miller, T.C., "Crack Growth Rates in a Propellant Under Various Conditions" (Paper)

JANNAF 34th Structures & Mechanical Behavior Subcommittee Meeting
(Cocoa Beach, FL, 26-30 Mar 01) (Deadline: 26 Mar 2001)

(Statement A)

Crack Growth Rates in a Propellant Under Various Conditions *

T. C. Miller

Air Force Research Laboratory

10 E. Saturn Blvd., Edwards AFB, California 93524

Abstract

Crack growth in a solid rocket propellant is detailed. Experimental studies at both ambient and pressurized conditions have been conducted, and results include crack growth data for different geometries at different pressures. Pressure slows the crack growth. This is related to the suppressing of microstructural void formation near the crack tip.

Introduction

Cracks may form in a solid rocket propellant during the manufacture, handling, storage, or use of the solid rocket motor. However, even after the formation of these cracks, the motor may still be usable, because the cracks may not grow under anticipated loads or may grow slowly enough to avoid catastrophic consequences before service life ends. During our examination of cracks in solid propellant, we have tried to answer two key questions: (i) at what point does a crack in propellant begin to grow, and (ii) after growth begins, at what rate does this growth occur? The answer to these questions is complex, and in this study we address some recent findings on the growth rate issue.

The crack growth in a solid propellant is complex because of three aspects of the phenomenon. First, propellant is a rubbery particulate composite that has unusual properties that have not been as thoroughly analyzed as other types of materials. The more widely developed fracture mechanics and mechanics of materials concepts are not necessarily easily applied to a propellant material. The second complication is also related to the makeup of the propellant - because of rate and temperature dependencies and extreme ductility, we cannot use conventional experimental approaches (e.g., strain gages) to measure the related variables. Lastly, the service conditions are varied. During long term storage, the mismatch of thermal expansion coefficients of the different materials (casing, insulator, liner, and propellant) induces stresses that can cause crack growth, resulting in low stresses experienced over an extremely long time. At the other extreme, the composite will experience a set of very high stresses due to pressure from the exhaust gases, and these high stress conditions will be held for a much smaller time.

Because of these complications, we cannot assume that the growth of cracks in propellant is independent of the many factors that exert little if any effect on conventional materials. The crack geometry, overall specimen geometry, loading rate, temperature, pressure, and other effects may all influence the speed at which the crack grows. We will obtain more accurate predictions, as the effect of these variables is examined. This work considers the effects of specimen and crack geometry and pressure effects.

*Approved for public release, distribution is unlimited

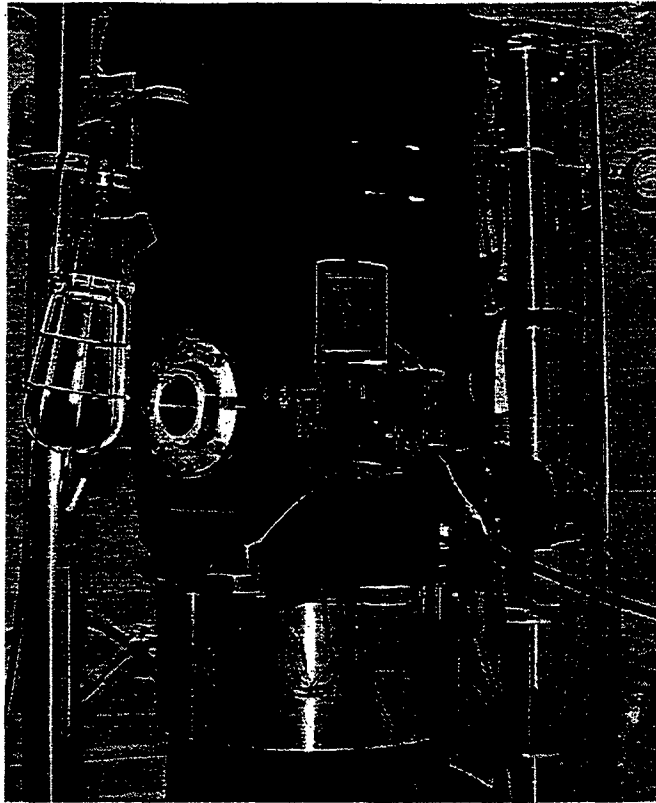


Figure 1: Test Chamber Used for Pressure Testing of Fracture Specimens

Experimental Procedures

We used two main testing sites to conduct our experiments. This was advantageous because the agreement of data collected from different sites gives us confidence that the results are reproducible under different laboratory conditions. However, for these experiments we required the alternate testing site because our facility at Edwards AFB did not have the pressure chamber we needed for the pressure experiments. Additional work has been done at other locations using even more specialized equipment.

The pressure chamber we used (see Figure 1) incorporates seals that allow the testing machine fixtures to be inside the chamber but the crosshead to be outside. We used sight ports so that we could see the specimen during testing. Nitrogen was used as the pressurizing gas because of its non-reactivity. The gas is ported into the sealed chamber and then the pressure and test temperature are stabilized. Test pressures of 1000 psi (6895 kPa) were used for comparison with ambient pressure results.

During the testing of some specimens (for example the single edge notched specimens) the specimen may rotate about the "hinge point" represented by the crack tip. With conventional materials the rotations would be insignificant and would not pose a problem, but with solid propellant the rotations can be excessive, requiring any related modeling efforts to incorporate nonlinear geometry effects. To solve this problem, we used rigid connectors at the pressure test facility to prevent rotations at the end of the specimens. At the ambient pressure facility, we achieved this by using another fixture that has guide rods that prevent the rotation of the specimen (see Figure 2).

For tests with crosshead speeds of 2 in/min (50.8 mm/min) or less, normal VHS equipment could be used to record the progress of fracture in the specimen. Above these speeds, high-speed video is required,



Figure 2: Fixture to Prevent End Rotations Used in Ambient Test Facility

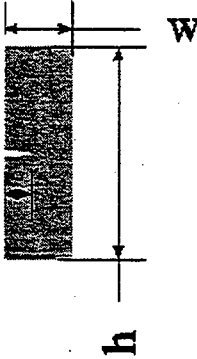
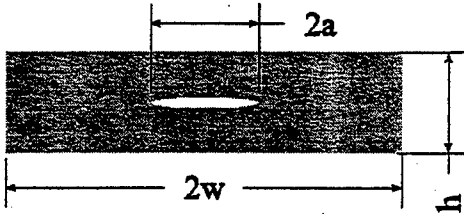
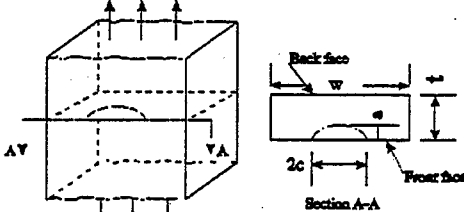
since the 30 frame/second conventional frame rate is not fast enough to sample the event adequately. In either case, we used CCD cameras and time code generators in series with the video recording equipment. The cameras record the image during fracture, and the time code generators print the time onto the videotape image to make later analysis easier.

During a typical procedure, we fabricated the specimen and cut a crack into the specimen. The surface cracked specimens were cut with a semicircular cutting blade made from a razor blade, but in other cases a normal razor blade was used to make the cut. We glued the specimens into end tabs with epoxy and set them in the loading assembly. For pressure conditions, the chamber was closed, pressurized, and allowed to stabilize. After this, we pulled the specimens with a constant crosshead speed and simultaneously recorded the crack growth on videotape. After this, the videotape data and the testing machine data were used to analyze the fracture event.

Table 1 shows the various tests reported in this work. There are four types of specimens used here. The most often used was the single edge notched tension (SENT) specimen. This is used frequently because of the ease of use. To examine the effects of thickness, we varied the specimen thickness. Specimen thicknesses of 0.2, 0.5, 1.0, and 1.5 inches (5.08, 12.7, 25.4, and 38.1 mm) were tested. The different thicknesses all gave similar results (a discussion of the reasons for this is beyond the scope of this work but is detailed in other works).[1] The crack size was also altered; crack sizes of 0.1 and 0.3 inches (2.54 and 7.62 mm) were studied. Biaxial test specimens have also been tested, and have been preferred in the past because the stress conditions near the crack are similar to those found in the rocket. The surface cracked specimens contained "thumbnail" cracks on one of their surfaces, and similar cracks may be found in actual motors.

After the test, we know the load and extension histories from the testing machine. The videotape is used to find the moment at which crack extension first occurs. The load at this time can be used to determine the stress intensity factor at initiation, K_{Ii} . We measured the crack size from this point until the attainment of maximum load at set intervals from the videotape clips. This can be done either directly from a monitor screen or by capturing the video sequences onto a computer and using software to determine the lengths;

Table 1: Test Matrix for Crack Growth Experiments

Specimen Type	Figure	Test Conditions
single edge notched tension	 <p data-bbox="520 810 954 995"> $w = 1 \text{ in (25.4 mm)}$ $a = 0.1, 0.3 \text{ in (2.54, 7.62 mm)}$ $h = 3, 5 \text{ in (76.2, 127 mm)}$ thickness = 0.2, 0.5, 1.0, 1.5 in (5.08, 12.7, 25.4, 38.1 mm) </p>	strain rate = 0.067 min^{-1} , ambient pressure, 1000 psi (6285 kPa) pressure
biaxial stress	 <p data-bbox="560 1257 900 1389"> $2w = 8 \text{ in (203.2 mm)}$ $2a = 1.5 \text{ in (38.1 mm)}$ $h = 2 \text{ in (50.8 mm)}$ thickness = 0.2 in (5.08 mm) </p>	strain rate = 0.1 min^{-1} , am- bient pressure
surface cracked	 <p data-bbox="571 1698 884 1789"> $a = c = 0.4 \text{ in (10.16 mm)}$ $t = w = 2 \text{ in (50.8 mm)}$ height = 2.75 in (69.85 mm) </p>	strain rate = 0.067 min^{-1} , 1000 psi (6285 kPa) pressure

the two methods have about the same accuracy. In some cases (for example, the single edge notched tension specimens) the crack length was indirectly measured by measuring the ligament size in front of the crack.

To analyze this data, the crack speed must be determined from this sporadic growth history. One way to do this is to use a secant method or the modified secant method to analyze the crack growth data. In our case, however, we were interested in relating the average crack speed to a fracture parameter, and the more appropriate method was to fit a polynomial curve to the crack size vs. time data. Taking the time derivative gives the crack speed at any moment in time.

The solid propellant consists of a high volume fraction of hard particles embedded in a soft rubbery matrix. When loaded, the loads at the crack tip intensify until damage occurs by voids nucleating from the hard particles and then growing and coalescing. The extreme ductility of the rubbery matrix produces ligaments that may bridge the crack in the area immediately behind the crack tip. Once enough damage accumulates before the crack tip, the crack advances by merging with the newly formed voids. This growth leaves the advancing crack tip in undamaged territory, and the process is repeated. These microstructural phenomena cause sporadic crack growth history, with the crack growth slowing or even stopping throughout the loading history.[2]

Fracture parameters must also be assessed. In this work, we used linear elastic fracture parameters. These depended on the load at any point in time, and can generally be expressed as:

$$K = \sigma \sqrt{\pi a} f(\text{geometry}) \quad (1)$$

From the measured data, crack size and load are known at any time, and the value of K can be calculated from these values using this equation. Here σ is the nominal stress, a is a crack size parameter, and f is a geometric correction factor. For the surface cracks, the specimen dimensions a and c were assumed equal throughout the fracture process. Also, the geometric correction factor depends on the ratio of the crack size to one or more of the specimen dimensions. For the SENT and the biaxial specimens, the crack size to width ratio, a/w , is the only relevant parameter, but for the surface cracked specimens, the width, thickness, and crack size are all involved.

The specific geometric correction factors are not detailed here, but are noted in other works.[1, 3, 4] They were derived from finite element analysis of the specific geometries or similar geometries with similar boundary conditions. Because of the nature of the loading, displacement boundary conditions were used when possible in the finite element analyses. For the surface cracks, geometric correction factors were obtained from a previous work by Newman and Raju.[4]

The crack speeds can be related to the stress intensity factor through a power law relationship:

$$\frac{da}{dt} = CK^m \quad (2)$$

This relationship has been used often in the past, and gives a way to predict the crack growth based on the crack size and anticipated loads in the actual structure.[1, 3, 5, 6, 7] The data for any set of conditions we tested is modeled reasonably using this approach. By comparing datasets for different test conditions, we can see the effects of various parameters (i.e., geometry and pressure).

Results and Discussion

Under ambient pressure conditions, we tested single edge notched tension (SENT) specimens and biaxial test specimens. Table 2 shows the comparison between the two specimens for similar specimen strain rates and conditions. From the table, it can be seen that the parameters for the crack growth equation agree well.

Table 2: Crack Growth Comparisons at Ambient Pressure for Different Specimen Geometries

$$\frac{da}{dt} = C_1 K_I^{C_2} \text{ or } \log\left(\frac{da}{dt}\right) = \log(C_1) + C_2 \log(K_I)$$

Specimen Type	$\log(C_1)$	C_2	da/dt (in/sec)	
			$K_I = 50 \text{ psi in}^{1/2}$	$K_I = 90 \text{ psi in}^{1/2}$
single edge notched tension	-6.030	2.084	0.0028	0.0110
biaxial stress	-6.590	2.375	0.0032	0.0113

The agreement is more clearly established by comparing the crack growth rates for the two specimens at representative values of 50 and 90 psi in^{1/2} (54.94 and 98.90 kPa m^{1/2}), and these are also given in the table. The implication is that for the purposes of calculating crack growth rates, either specimen can be used.

Comparison with other specimen geometries has been studied, and with similar results – the crack growth predictions are not significantly affected by the experimenter’s choice of geometry. This was true for the propellant tested here, and for another material that we previously tested. This conclusion should simplify future experimental procedures. We discovered that the crack growth rates were robust with respect to specimen geometry choices under pressurized conditions as well. Figure 3 shows the crack growth rate plots for 1000 psi (6895 kPa) pressure specimens and for the ambient pressure SENT specimens. The data for the two types of specimens (SENT and surface cracked specimens) tested under pressure agree well and even overlap to some extent. The conclusion is that the simpler SENT experiments can be used to predict the growth rates for the surface cracked specimens.

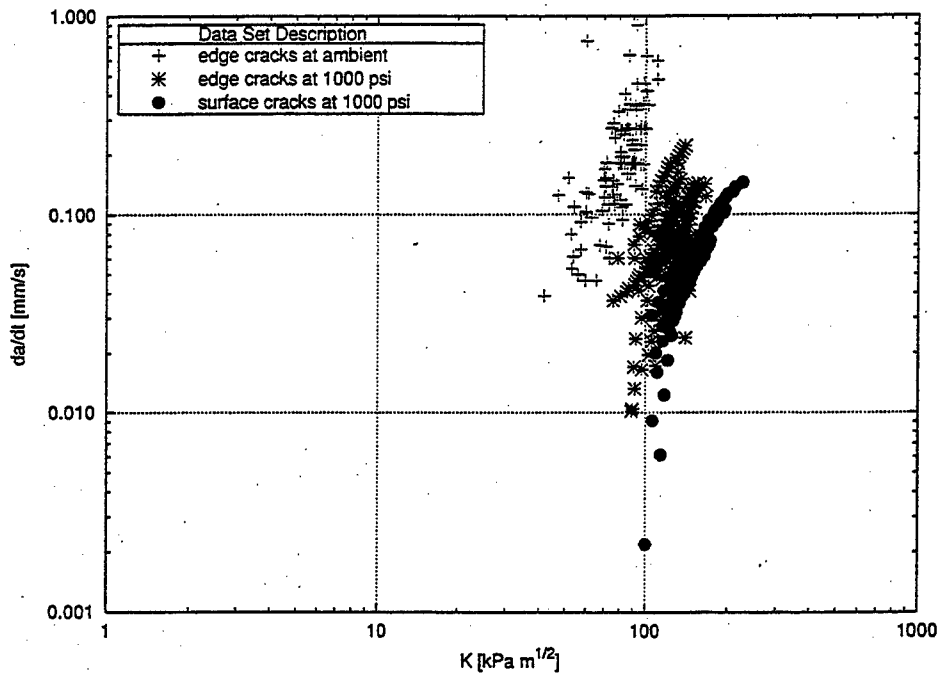


Figure 3: Crack Growth Results for Specimens Under Various Conditions

The comparison of the ambient pressure data with the 1000 psi (6895 kPa) data shows that the cracks tested under ambient pressure grow faster for the same level of stress intensity. This is explained by the microstructural phenomena that accompany crack growth. As explained in Experimental Procedures, the crack growth takes place by void nucleation, growth, and coalescence. These damage phenomena are strongly

affected by the hydrostatic component of the stresses surrounding the particles. The reason the damage occurs readily at the crack tip is that of the large hydrostatic component of stress created by the presence of the crack tip. The application of pressure to the specimen, however, superposes a negative component of hydrostatic stress onto the existing positive component, lowering the overall hydrostatic stress component.

A reduction of crack growth rates with pressure is good news because under service conditions the high pressures experienced inside the solid rocket motor help to slow the growth rate. Another implication is that for these anticipated conditions, the fracture testing of specimens should be done under pressure to prevent making overconservative predictions of growth rates.

Summary and Conclusions

For the conditions tested, specimen geometry and crack geometry did not significantly affect crack growth in the solid propellant. Biaxial test specimens gave similar results to single edge notched tension specimens, as did surface cracked specimens. This robustness did not change with the application of pressure. The effect of pressure, however, was significant, and caused a slowing of the crack growth for identical stress intensities. This slowing is due to the pressure affecting the hydrostatic component of stress near the crack tip, which in turn affects the microstructural phenomena of void nucleation, growth, and coalescence.

The results could be useful in several ways. First, the results help us to formulate experimental procedures – the experimenter can be less concerned with specimen geometry, but should be careful to use growth data with pressure conditions similar to those anticipated in service. Regarding applications, once the crack growth rates are found, they can be compared with the burn rate in the propellant. If the burn rate exceeds the crack growth rate, it is likely that the crack will burn up before catastrophic failure. With only growth initiation data, the researcher may be forced to make overly conservative predictions. Conversely, the researcher with crack growth data can make predictions that save hardware and result in millions of dollars in cost savings. There may be other uses for crack growth rate predictions not explored here. For example, once the parameters in equation 2 are determined, integral calculus can be used to determine the initial crack size existing in the solid propellant. One researcher has done this and confirmed the results with several other experimental methods. If the initial crack size can be determined using only this simple data, then more difficult experimental methods can be avoided. This initial crack size estimation is important to the rocket industry for the specification of sensitivity in nondestructive inspection techniques.

References

- [1] Miller, T. C. and Liu, C. T., *The Effects of Pressure on Fracture of a Rubbery Particulate Composite*, Proceedings of the Society for Experimental Mechanics IX International Congress and Exposition, Orlando, Florida, 792-795 (2000).
- [2] Liu, C. T., *Critical Analysis of Crack Growth Data*, Journal of Propulsion, 6(5), 519-524 (1990).
- [3] Miller, T. C. and Liu, C. T., *Pressure Effects and Fracture of a Rubbery Particulate Composite*, Experimental Mechanics, , submitted for publication (2000).
- [4] Newman, J. C., Jr., *A Review and Assessment of the Stress-Intensity Factors for Surface Cracks*, in Special Technical Publication 687: Part- Through Crack Fatigue Life Prediction, J. B. Chang, ed., American Society for Testing and Materials, 16-42 (1979).
- [5] Baron, D. T., Miller, T. C. and Liu, C. T., *Subcritical Crack Growth in a Composite Solid Propellant*, Journal of Reinforced Polymer Composites, 18(3), 233-250 (1999).
- [6] Miller, T. C., *Mixed-Mode Fracture in a Rubbery Particulate Composite*, Sixth International Conference on Composites Engineering, Orlando, Florida, 575-576 (1999).

- [7] Liu, C. T. and Miller, T. C., *Effect of Crack Size on Initiation and Growth Behavior in a Particulate Composite Material*, Proceedings of the Society for Experimental Mechanics IX International Congress and Exposition, Orlando, Florida, 1017-1020 (2000).